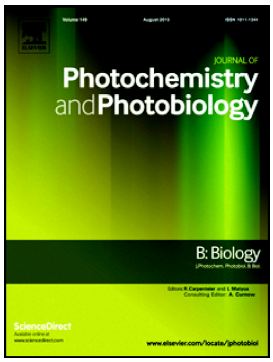

BODIPYs bearing a dimethylaminopropoxy substituent for imaging and photodynamic inactivation of bacteria

Yohana B. Palacios, Sofia C. Santamarina, Javier E. Durantini, Edgardo N. Durantini, Andrés M. Durantini

PII: S1011-1344(20)30499-1

DOI: https://doi.org/10.1016/j.jphotobiol.2020.112049

Reference: JPB 112049

To appear in: *Journal of Photochemistry & Photobiology, B: Biology*

Received date: 23 June 2020

Revised date: 29 September 2020

Accepted date: 4 October 2020

Please cite this article as: Y.B. Palacios, S.C. Santamarina, J.E. Durantini, et al., BODIPYs bearing a dimethylaminopropoxy substituent for imaging and photodynamic inactivation of bacteria, *Journal of Photochemistry & Photobiology, B: Biology* (2020), https://doi.org/10.1016/j.jphotobiol.2020.112049

BODIPYs bearing a dimethylaminopropoxy substituent for imaging and photodynamic inactivation of bacteria

Yohana B. Palacios[1,†], Sofia C. Santamarina[1,†], Javier E. Durantini[2], Edgardo N. Durantini[1] and Andrés M. Durantini[1,*]

[1]*IDAS-CONICET, Departamento de Química, Facultad de Ciencias Exactas, Físico-Químicas y Naturales, Universidad Nacional de Río Cuarto, Ruta Nacional 36 Km 601, X5804BYA Río Cuarto, Córdoba, Argentina.*

[2]*IITEMA-CONICET, Departamento de Química, Facultad de Ciencias Exactas, Físico-Químicas y Naturales, Universidad Nacional de Río Cuarto, Ruta Nacional 36 Km 601, X5804BYA Río Cuarto, Córdoba, Argentina*

* Corresponding author.

† These authors contributed equally to this work.

Abstract

A new BODIPY (BDP 1) bearing a dimethylaminopropoxy group attached to a phenylene unit was synthesized. This compound was brominated to obtain the halogenated analog BDP 2, which was designed to enhance the photodynamic effect of BODIPY to kill bacteria without an intrinsic cationic charge. The basic amino group located at the end of the propoxy bridge can acquire positive charge by protonation in an aqueous medium, increasing the binding to bacterial cells. Interaction and photokilling activity mediated by these compounds was evaluated in *Staphylococcus aureus* and *Escherichia coli*. BDP 1 and BDP 2 were rapidly bound to bacterial cells, showing bioimages with green emission. Complete elimination of *S. aureus* was detected when cells were incubated with 1 μM BDP 2 and irradiated for 5 min. Comparable photoinactivation was obtained with *E. coli*, after an irradiation of 30 min. Furthermore, BDP 2 was effective to kill bacteria at very low concentration (0.5 μM). Thus, BDP 1 showed mainly interesting properties as a fluorophore, whereas BDP 2 was highly effective photosensitizer as a broad-spectrum antibacterial agent.

Keywords: BODIPY; photosensitizer; fluorophore; photodynamic inactivation; bacteria.

1. Introduction

The increased resistance of bacteria to antibiotics for clinical use makes it difficult to cure many infectious diseases [1]. The overuse of antimicrobials in hospitals as a prophylactic measure in surgical operations, the tendency to use broad-spectrum antibiotics, self-medication, inadequate prescription and non-compliance with treatments by patients are some of the factors responsible for mutagenic changes in these pathogenic microorganisms. Also, the resistance can be increased by the use of antibiotics for multiple purposes in the husbandry of livestock [2]. The Gram-positive bacteria *Staphylococcus aureus* has been recognized as one of the pathogens with the highest epidemiological resistance found in hospital treatments [3]. Consequently, this microorganism represents a serious threat to medicine in health care. Also noteworthy is the worldwide presence of Gram-negative bacteria resistant to multiple drugs, such as *Escherichia coli* to different generations of antibiotics [4]. A significant number of serious nosocomial infections are caused by *E. coli* [5]. Furthermore, this bacterium is part of a significant reservoir in animals, as well as in the environment [6]. Despite the constant expansion of antibiotic resistance, the number of new antimicrobial agents to be used as medications has been quite limited in recent years. Therefore, the development of substitute strategies is required to ensure that bacterial diseases continue treatable with accessible therapies [7]. One of the therapies that have been proposed to eradicate resistant microorganisms is known as photodynamic inactivation (PDI) [8]. This is a promising method that is based on the formation of reactive oxygen species (ROS) by a photosensitizer (PS), which was previously incorporated into microbial cells. After excitation of the PS with appropriate light, two photodynamic pathways can occur in PDI [9]. Type I process involves the PS excited triplet state that reacts with different substrates by electron or proton transfer, leading to the formation of free radicals. These highly reactive intermediates can interact with molecular oxygen in the ground state ($O_2(^3\Sigma_g^-)$) to produce ROS, such as hydroxyl radical ($HO^\bullet$), superoxide anion radical ($O_2^{\bullet-}$), and hydrogen peroxide (H_2O_2). On the other hand, the PS excited triplet state can form singlet molecular oxygen, $O_2(^1\Delta_g)$, by energy transfer in a type II pathway [10]. During the therapy, these

mechanisms can occur independently or combined depending on the PS and the medium. Either way, ROS is produced and react rapidly with various biological components inducing microbial cells death.

In the last decade, numerous PSs have been studied and evaluated as phototherapeutic compounds for the PDI of microorganisms. However, there are relatively few structures derived from 4,4-difluoro-4-bora-3a,4a-diaza-*s*-indacene (BODIPY) proposed as PSs for the photoinactivation of microorganisms [11]. The synthesis of these derivatives offers a wide range of alternatives to attach different substituents, as well as the versatility to produce modifications in the periphery of the *s*-indacene ring [12]. This family of compounds has very interesting spectroscopic properties, including a high molar absorption coefficient and fluorescence emission in the central region of the visible spectrum. For this reason, together with their good photochemical stability, these compounds have originally been proposed as fluorophores for bioimaging [13]. BODIPY core has been subsequently improved to decrease fluorescence emission and increase the formation of excited triplet state for applications in photodynamic therapy [14].

The aim of this investigation was to synthesize new BODIPY derivatives containing a dimethylaminopropoxy group attached to the phenylene unit. BDP 1 was designed to act primarily as a fluorophore, while brominated BDP 2 as a potential phototherapeutic agent for the inactivation of bacteria. In previous studies, a BODIPY substituted by trimethylaminopropoxy group with intrinsic positive charges in combination with potassium iodide was effective as a broad-spectrum antimicrobial PS [15,16]. Furthermore, porphyrins and chlorins showed that the presence of dimethylaminopropoxy groups on the periphery of the macrocycle turns these compounds into effective PSs to inactivate microorganisms [17,18]. This substituent bears a basic amine group that can acquire positive charges in aqueous media, improving the interaction of PS with the cell envelope. In addition, spectroscopic characteristics and photodynamic properties of these BODIPYs were determined in homogeneous media. Moreover, photosensitized production of $O_2(^1\Delta_g)$ and ($O_2^{\bullet-}$) mediated by both BODIPYS was evaluated in the presence of different molecular sensors to

detect ROS. Studies in biological cultures were carried out in a typical Gram-positive bacteria *S. aureus* and Gram-negative bacteria *E. coli*. These investigations were focused on the ability of these compounds for imaging fluorescent bacterial cells and photokill pathogens.

2. Materials and methods

2.1. Synthesis of BODIPY derivatives

8-Acetoxymethyl-1,3,5,7-tetramethyl pyrromethene fluoroborate (H_2B-OAc) and 8-acetoxymethyl-2,6-dibromo-1,3,5,7-tetramethyl pyrromethene fluoroborate (Br_2B-OAc) were synthesized as previously reported [19].

4,4-Difluoro-8-[4-(3-(*N*,*N*-dimethylamino))propoxiphenyl]-1,3,5,7-tetramethyl-4-bora-3a,4a-diaza-*s*-indacene (BDP 1). 2,4-Dimethylpyrrole (500 µL, 4.85 mmol) and 4-(3-(*N*,*N*-dimethylamino)propoxy)benzaldehyde (400 µL, 1.65 mmol) were treated with trifluoroacetic acid (TFA, 30 µL, 0.39 mmol) in 75 mL of dichloromethane (DCM). The solution was deoxygenated with argon and stirred overnight at room temperature. Then, 2,3-dichloro-5,6-dicyano-1,4-benzoquinone (DDQ, 461 mg, 2.03 mmol) in 25 mL of DCM was added drop by drop in the reaction flask and the mixture was kept under stirring for 6 h. After that, it was placed in a cold bath to decrease the temperature to about -1° C and an excess of triethylamine (TEA, 5 mL, 35.9 mmol) was incorporated and boron trifluoride diethyl etherate (BF_3·OEt_2, 5 mL, 40.5 mmol) was added after 15 min and the solution was stirred for 12 h. The mixture was washed with water and the organic phase was dried over Na_2SO_4. The crude product was obtained by solvent evaporation under reduced pressure. The product was purified by flash column chromatography (silica gel) using DCM:*n*-hexane (80:20) with 1% TEA as eluent provided 127 mg (14%) of BDP 1. TLC (DCM: TEA 1%) R_f = 0.54. ^{1}HNMR ($CDCl_3$, TMS) δ [ppm] 1.49 (s, 6H), 1.96 (m, 2H), 2.30 (s, 6H, -N(CH_3)$_3$), 2.51 (t, 2H, *J* = 6.8 Hz, -CH_2-N), 2.55 (s, 6H), 4.11 (t, 2H, *J* = 6.1 Hz, -CH_2-O), 5.97 (s, 2H, pyrrole), 7.00 (d, 2H, *J* = 8.7 Hz, Ar), 7.17 (d, 2H, *J* = 8.7 Hz, Ar). ESI-MS [m/z] 426.2521 (425.2528 calculated for $(M+H)^+$, M = $C_{24}H_{30}BF_2N_3O$).

2,6-Dibromo-4,4-difluoro-8-[4-(3-(*N*,*N*-dimethylamino))propoxiphenyl]-1,3,5,7-tetramethyl-4-bora-3a,4a-diaza-*s*-indacene (BDP 2). A mixture of BDP 1 (28 mg, 0.065 mmol) and *N*-bromosuccinimide (NBS, 25 mg, 0.14 mmol) in 3 mL of (trifluoromethyl)benzene (TFB) was stirred for 25 min at room temperature. The organic solution was washed with water and dried over Na_2SO_4. Finally, TFB was removed by distillation under reduced pressure. Flash column chromatography (silica gel) using DCM:*n*-hexane (80:20) with 1% TEA as eluent afforded 37 mg (98%) of BDP 2. TLC (DCM:TEA 1%) R_f = 0.50. ^{1}HNMR ($CDCl_3$, TMS) δ [ppm] 1.43 (s, 6H), 1.99 (m, 6H), 2.31 (s, 6H, -N(CH_3)$_3$), 2.52 (t, 2H, *J* = 6.8 Hz, -CH_2-N), 2.60 (s, 6H), 4.12 (t, 2H, *J* = 6,1 Hz, -CH_2-O), 7.01 (d, 2H, *J* = 8.8 Hz, Ar), 7.16 (d, 2H, *J* = 8.8 Hz, Ar). ESI-MS [m/z] 582.0741 (582.0738 calculated for $(M+H)^+$, M = $C_{24}H_{28}BBr_2F_2N_3O$).

2.2. Spectroscopic measurements

UV-visible absorption and fluorescence studies were performed as reported [15]. Spectral determinations were achieved using 1 cm path length quartz cells in acetonitrile (ACN) at room temperature. To obtain the emission spectra, absorbances (<0.05) of the samples were matched at the excitation wavelength (λ_{exc} = 490 nm). The areas of the fluorescence intensity *vs*. wavelength were integrated in the range of 495-800 nm. The fluorescence quantum yield (Φ_F) of BODIPYs were calculated taking into account the area below the corrected emission spectrum with that of H_2B-OAc, which was as a reference (Φ_F = 0.87 in ACN) [19].

2.3. Computational details

All density functional theory (DFT) computations were attained with a Gaussian 09 package (Gaussian, Wallingford, CT) using the B3LYP functional coupled with the 6-31G(d) basis set [20]. Geometries for the molecules were fully optimized. Conformational searches were achieved to locate the minimum-energy conformers of the molecules. Originally, numerous geometries were produced by the conformational search modules of Spartan'14 (Wavefunction, Inc., Irvine.) using

MMFF force field and then subjected to PM6 optimization. All molecular structures were consecutively re-optimized at the B3LYP/6- 31 G(d) levels of theory. Optimized structures in the excited singlet state were obtained by geometry optimizations performed using the TD-DFT method. Molecular electrostatic potential (ESP) surfaces of the optimized structures were visualized using GaussView Software Version 6.0, with an iso value of 0.0004 e/au^3. The colors of the potential surfaces were selected to obtain the maximum contrast between the relative locations of the positive (blue) and negative (red) charges.

2.4. Determination of $O_2(^1\Delta_g)$ formation

DMA (35 µM) and BODIPY (absorbance 0.1 at 506 nm) in 2 mL ACN were irradiated with light at λ_{irr} = 506 ± 6 nm under aerobic conditions. Photooxidation of DMA was measured by the decrease of the absorbance (A) at λ_{max}=378 nm [15]. Fit of the semilogarithmic plot of ln A_0/A *vs.* time using linear least-squares was used to calculated the observed rate constants (k_{obs}) values. Under the same experimental conditions, quantum yields of $O_2(^1\Delta_g)$ production (Φ_Δ) in ACN were determined by comparing the k_{obs} for the corresponding BODIPY with that of Br_2B-OAc, which was used as a reference (Φ_Δ = 0.79 in ACN) [19].

2.5. Photoreduction of nitrotetrazolium blue (NBT)

Aerobic solutions of NBT (0.2 mM), β-NADH (0.5 mM) and BODIPY (absorbance 0.1 at 506 nm) in 2 mL of DMF/1% water were exposed with light at λ_{irr} = 506 ± 6 nm. The decomposition of NBT was monitored by increasing absorbance at λ = 560 nm due to the formation of diformazan [20]. Controls were carried out in the absence of each of the components.

2.6. Bacterial strains and cultures

S. aureus ATCC 25923 and *E. coli* EC7 strains were used in this investigation [16,17]. Cultivation and handling of bacteria to yield ~10^8 colony forming units (CFU)/mL in phosphate-

buffered saline (PBS, pH = 7.0) were attained as reported (see supporting information) [16]. Viable bacteria were calculated by spread plate method using serial dilutions 10-fold in PBS after an incubation of the culture for 24 h at 37 °C in the dark.

2.7. Binding of BODIPYs to bacterial cells

Bacterial cells (2 mL, ~10^8 CFU/mL) in Pyrex culture tubes (13 × 100 mm) were treated with BDP 1 or BDP 2 in the dark at 37 °C, varying the PS concentrations (0.5 and 1.0 μM) and incubation times (2, 5, 15 and 30 min). The BODIPYs were added to the cultures from a stock solution (0.5 mM) in ACN. In each experiment, 1 mL of the cell suspension was placed in an Eppendorf tube. After that, cells were harvested by centrifugation for 1 min at 14,000 rpm and the pellets were re-suspended in 3 mL of 2% aqueous sodium dodecyl sulfate (SDS). Samples were kept overnight at 4 °C in dark and then sonicated for 15 min. Fluorescence intensity of each BODIPY in the supernatant was measured by spectrofluorimetry (λ_{exc} = 480 nm, λ_{em} = 510 nm for BDP 1 and λ_{exc} = 480 nm, λ_{em} = 536 nm for BDP 2, Figure S1 and S2). The concentration of the PS in the solution was determined using a calibration curve, which was obtained using standard solutions (0.005-0.2 μM) of the BODIPY in 2% SDS. The amount of BODIPY bound to the cells was calculated considering the total number of cells [16].

2.8. Fluorescence images of attached bacterial cells

Fluorescence microscopy images were completed using the procedure reported [21,22]. Bacterial suspension (100 μL) was incubated in a chamber, formed by a polymeric cylinder glue to a coverslip, for 30 min at 37 ºC to allow the cells to anchor to the glass surface. Then, the chamber was washed with PBS to remove bacterial cells that were not attached to the glass. After that, 1 μM BOBIPY in 200 μL PBS was added into the chamber and kept in the dark for 30 min in dark at 37 ºC. Cells were washed with PBS to remove the PS that was not bound to cells and fluorescence images were taken under a microscope.

2.9. Photosensitized inactivation of bacterial cells

Bacteria in PBS (1 mL, ~10^8 CFU/mL) were treated with each BODIPY using different concentrations (0.5 and 1.0 μM for *S. aureus* and 0.5, 1.0 and 5.0 μM for *E. coli*) for 30 min in the dark at 37 °C [16]. Then, the cell suspensions were irradiated with visible light (70 mW/cm^2) in 96-well microtiter plate for different periods (2, 5 and 15 min for *S. aureus* and 5, 15 and 30 min for *E. coli*). The amount of viable bacterial cells was calculated as described above. In all biological tests, controls and statistical analysis with bacterial cells were performed as reported (see supporting information) [16].

3. Results and discussion

3.1. Synthesis of BODIPYs

The synthetic approaches to obtain the BODIPYs are illustrated in Scheme 1. BDP 1 was synthesized from 4-[3-(*N*,*N*-dimethylamino)propoxy]benzaldehyde and 2,4-dimethylpyrrole catalyzed by TFA in DCM. In the first stage, this reaction yielded the corresponding dipyrromethane substituted with a dimethylaminopropoxyfenil group at the central position of *s*-indacene ring (*meso* position).

The dipyrromethane was aromatized with DDQ to produce its counterpart dipyrromethene, which was changed to a BODIPY core by complexation with a difluoroboryl unit through reaction with $BF_3{\cdot}OEt_2$ using TEA as a basic catalyst [23]. For the preparation of the brominated derivative BDP 2, an aromatic electrophilic substitution was carried out at positions 2 and 6 of BDP 1 with NBS in TFT (Scheme 1). The use of NBS in fluorinated solvents (TFT) drastically reduces the reaction time of halogenations giving excellent yields and regioselectivity to positions 2 and 6 of BODIPY core [21,24]. Both products were purified by chromatography on silica gel, yielding 14% and 98% of BDP 1 and BDP 2, respectively.

BDP 1 and BDP 2 do not have an intrinsic positive charge on their phenylene substituent. Nevertheless, these BODIPYs contain in the *meso* position a basic amino group that act as precursors of positive charges on the periphery of the chromophore. Considering the basicity of the aliphatic amine groups (3-*N*,*N*-dimethylaminepropanol, pK_a = 9.51) protonation of this substituent is expected in PBS [25]. Furthermore, the formed cationic center is isolated from the BODIPY structure by an aliphatic chain. Optimized structure and ESP surfaces of BDP 1 and BDP 2 were compared with those of their protonated forms as shown in Figure 1. From this analysis, spatial regions in the molecular structure were determined in which the molecular electrostatic potential was negative and positive. This allowed us to visualize the charged regions of each molecule and the distribution on the structure of the BODIPY. As can be seen, the cationic charge does not have a significant effect on the electronic density of the BODIPY nucleus. Therefore, this isolation of the cationic group allows to retain the spectroscopic and photodynamic properties of PS. In addition, the aliphatic spacer in the aryl substituent provides higher mobility of the charged group, which can facilitate the binding of the PS to bacterial cells increasing its PDI activity [17,18].

3.2. Absorption and fluorescence spectroscopic properties

The UV-visible absorption spectra of BDP 1 and BDP 2 in ACN are shown in Figure 2A. The spectra of these compounds presented the characteristic bands of BODIPYs with similar structures [26]. The spectroscopic properties of these BODIPYs are given in Table 1. The main band of the non-halogenated dye was centered at ~ 500 nm. This band corresponds to the vibratory band 0-0 of the transition to the first excited state ($S_0 \rightarrow S_1$) [15]. A small characteristic shoulder at a shorter wavelength centered around 475 nm was observed, which was assigned to the 0-1 vibrational band of the same electronic transition. In addition, a second small band displaced to blue (~ 370 nm) was detected that was attributed to the transition $S_0 \rightarrow S_2$. In BDP 2, the presence of bromine atoms at positions 2 and 6 of BODIPY core produced a bathochromic shift of 25 nm respect to BDP 1. Similar behavior on the main absorption was previously found for the

bromination of BODIPY derivatives [27]. This effect was assigned to the resonance donating effect of bromine atoms [19]. In both cases, sharp absorption bands were obtained indicating that these compounds are mainly non-aggregated in ACN.

Fluorescence emission spectra of BDP 1 and BDP 2 were performed in ACN (Figure 2B). BDP 1 presented a band around 506 nm that is characteristic for similar BODIPYs, while BDP 2 showed a fluorescence peak at 537 nm [27]. In this structure, the substitution with bromine atoms resulted in a bathochromic change of 31 nm in the emission spectra due to the effect of resonance donation of the heavy atoms. These emission bands were assigned to the 0-0 vibrational band of the $S_1 \rightarrow S_0$ transitions [15,28]. Furthermore, the energy levels of the singlet excited state (E_s) of these BODIPYs were determined considering the energy of the 0-0 electronic transitions (Table 1) [19]. Moreover, Stokes shifts of 9 nm for BDP 1 and 15 nm for BDP 2 were estimated from the difference between the positions of the maxima of the absorption and emission bands for the electronic transition 0-0. These small Stokes shifts show that the BODIPY structure does not change significantly after excitation [29]. Values of Φ_F for BDP 1 and BDP 2 were determined in ACN (Table 1). A higher Φ_F was found for BDP 1, which agrees with those previously reported for similar BODIPYs [27]. A 3.5-fold drop in Φ_F values was noted when comparing BDP 1 and BDP 2. The weak emission of BDP 2 was attributed to the substitution with bromine atoms, as found for this type of BODIPYs [19,27]. In a previous work, we have shown that the presence of bromine atoms at positions 2 and 6 of the *s*-indacene ring produces a 4-6-fold reduction in the fluorescence lifetimes due to the heavy atom effect showing a triplet state lifetime of ~40 μs [19]. This effect enhances spin-orbit coupling facilitating ISC and increasing the triplet state quantum yield [27,30]. For the non-halogenated analogues time resolution was not possible due to low phosphorescence emission.

The optimized structures of the BDP 1 and BDP 2 are shown in Figure 3. The BODIPYs were optimized to a stationary point on the Born-Oppenheimer potential energy surface of the molecules. The BODIPY entity was flat and the phenylene unit in an almost perpendicular

arrangement. Similar arrangement was determined in BDP 1-H^+ and BDP 2-H^+ protonated molecules (Figure S3). Electronic density calculations for BDP 1 and BDP 2 (Figure 3) indicated that the HOMO was positioned on the BODIPY core and the LUMO was also located in the *s*-indacene ring. Therefore, according to the theoretical calculations for these compounds the lowest-lying state $S_0 \rightarrow S_1$ excitation is almost completely associated with the HOMO/LUMO transition of the π-system [11,26]. This behavior is also expected in their protonated forms (Figure S3). Moreover, to evaluate the behavior of these BODIPYs after excitation with visible light, energy of HOMO and LUMO levels of exited state of BODIPY core and ground state of benzene derivatives were calculated (Figure S4). It was found that PeT process can take place from the dimethylaminopropoxybenzyl group towards brominated BODIPY unit but protonation of the amine group can avoid this process. Furthermore, charge distribution BDP 1-H^+ and BDP 2-H^+ protonated forms were slight affected in the excited singlet state respect to ground state, with the positive charge in the ammonium group localized at the end of the carbon chain (Figure 1).

3.3. Photosensitized generation of $O_2(^1\Delta_g)$

Aerobic photooxidation reaction of DMA induced by BDP 1 and BDP 2 was evaluated in ACN. The decrease in the concentration of DMA due to generation of endoperoxide was determined by reducing the absorbance at λ_{max} = 378 nm (Figure S5) [31]. Furthermore, the absorbance of the BODIPYs did not change after irradiation during the experiments, indicating a high photostability under these experimental conditions. Figure 4 shows characteristic plots that describe the consumption of DMA as the photooxidation reaction proceeds. Data plotted of ln A_0/A vs time are linear from which k_{obs}^{DMA} can be determined. These results are gathered in Table 1. The photooxidation rate of DMA mediated by BDP 1 was considerably lower (33-fold) than that sensitized by BDP 2.

From the kinetic data of DMA decomposition, the value of Φ_Δ was determined in ACN, using Br_2B-OAc as a reference [19]. This anthracene derivative mainly quenches $O_2(^1\Delta_g)$ by

chemical reaction. Therefore, DMA can be used to specifically detect and quantified the presence of this ROS [31]. Thus, values of Φ_Δ were calculated by comparing the k_{obs}^{DMA} (Table 1) for both BODIPYs with that for the reference. According with this approach, very low production of $O_2(^1\Delta_g)$ was detected using BDP 1 as PS [15,27]. In contrast, the effect of heavy atom in BDP 2 induced the formation of $O_2(^1\Delta_g)$ with similar value to those reported before for brominates BODIPYs [14,19].

3.4. Photoinduced production of $O_2^{\bullet-}$

Formation of $O_2^{\bullet-}$ was evaluated using NBT method with the addition of β-NADH [20]. The reaction of $O_2^{\bullet-}$ with NBT yields the reduction product diformazan, which has an absorption band centered at 560 nm. Thus, the aerobic decomposition of NBT sensitized by BDP 1 and BDP 2 were studied using β-NADH as reductant in solution of DMF/1% water. The changes in the absorption at 560 nm as a function of time are shown in Figure 5. A slow reduction of NBT mediated by these BODIPYS was observed in the absence of β-NADH. Likewise, a slight decomposition of NBT was found in presence of β-NADH without the BODIPYs. In contrast, the reaction of NBT increased when BDP 1 or BDP 2 and β-NADH were added in comparison with the solution without the BODIPY. In both cases, β-NADH was necessary for photosensitized generation of diformazan. The formation of $O_2^{\bullet-}$ was higher for the reaction photoinduced by BDP 1 than BDP 2. The ability of several related BODIPYs to generate $O_2^{\bullet-}$ was previously reported [27]. The formation of $O_2^{\bullet-}$ was more efficient for an unsubstituted BODIPY than for its brominated analog and even less for iodinated, in reverse order of $O_2(^1\Delta_g)$ production. In the case of BDP 1, the photodynamic action mainly involves the generation $O_2^{\bullet-}$ using β-NADH as reductant, while BDP 2 exerts its action by forming $O_2(^1\Delta_g)$ by a type II mechanism, according with the heavy atom effect.

3.5. Uptake of BODIPYs by bacteria

The capability of BDP 1 and BDP 2 to be incorporate by bacterial cells was studied in *S. aureus* and *E. coli*. Cell suspensions were treated with different BODIPY concentrations (0.5 μM

and 1.0 μM) in the dark at 37 °C. Figure 6 shows the amount of BODIPY recovered from bacterial cells after different incubation time (2, 5, 15 and 30 min). The highest binding values of BDP 1 and BDP 2 to microbial cells were quickly reached after 2 min of incubation. Furthermore, the amount of cell-bound BODIPY was not significantly changed incubating the bacterial cells for longer times (30 min). In *S. aureus*, the amount of recovered BODIPY was slightly higher for BDP 1 than BDP 2, while a similar uptake was found in *E. coli*. When *S. aureus* cells were incubated with 1.0 μM, an average value of 0.60 nmol/10^8 cells was obtained for BDP 1, while the uptake was 0.54 nmol/10^8 cells for BDP 2 (Figure 6A). In *E. coli*, the binding of both BODIPYs reached 0.51 nmol/10^8 cells (Figure 6B). In both bacterial strains, the number of molecules was reduced by approximately half when cultures were incubated with 0.5 μM of the BODIPYs. Therefore, non-saturation occurs over this concentration range. These results specify a high interaction between both BODIPYs and the pathogens. The presence of a positively charged precursor group allows a fast-cellular uptake in only 2 min of treatment. As already shown, cationic molecules can interact better with negatively charged components present in the cell wall. Comparable results were previously found with cationic BODIPYs bound to *S. aureus* and *E. coli* cells [16]. Moreover, this behavior was previously observed in the uptake of BODIPYs by bacteria [21]. In the present results for both bacteria, the cell-bound PS was similar, being slightly higher for BDP 1 than BDP 2 in *S. aureus*. The efficacy of PDI can be significantly influenced by the uptake of PSs by bacterial cells [32]. In Gram-negative bacteria, the outer membrane (OM) acts as a barrier to prevent the interaction of ROS with vital target components. The presence of lipopolysaccharides in OM affords a density of negative charges on bacteria. This anionic cell surface avoids the uptake of neutral and anionic PSs. Hence, combination in the PS structure of cationic groups with an amphiphilic character can be required for an effective inactivation of Gram-negative bacteria [18].

To obtain evidence on the cellular imaging of bacteria, fluorescence microscopy was used to evaluate the uptake of BDP 1 and BDP 2 by cells following a similar procedure previously described by us and others [21]. In this procedure, bacterial suspensions are incubated for 30 min in

a closed chamber. During this period, cells can attach to the glass surface thanks to its pilus. Then, planktonic microbes are eliminated by washing, remaining only those that were anchored to the glass. For the uptake experiments, 1 μM of the corresponding BODIPY in PBS was added in the chamber and fluorescence images were monitored as a function of time. A fast binding of BODIPY to either *S. aureus* or *E. coli* was found observing the green fluorescence emission of the bacterial cells. This is illustrated in Figure 7A for bacteria treated with BDP 1. As can be observed, emission in the green channel corresponding to BDP1 was detected for both bacteria indicating the uptake of this BODIPY. The fluorescent images were also noticed in cells treated with BDP 2 (Figure 7B). However, a considerably less intense emission was found for cells treated with the brominated BODIPY. This fact coincides with the lower Φ_F of BDP 2 than BDP 1, attributed to fluorescence quenching due to the heavy atom effect that promotes intersystem crossing. Similar results were previously reported for cationic BODIPYs bound to microbial cells [16]. The emission shown mainly by BDP 1 in the biological environment indicates that this compound has interesting characteristics to be used as a fluorophore for cell diagnostic images.

3.6. PDI of bacteria

The photodynamic activity sensitized by BDP 1 and BDP 2 was evaluated for *in vitro* inactivation of *S. aureus* and *E. coli* cells. Several strains of *S. aureus* have developed resistance to multiple drugs due to adaptation to different antibiotics, with few possible therapies available for their treatment [33]. Furthermore, this microbe has been described as the main human pathogen that causes hospital-acquired infections [3]. For PDI studies, *S. aureus* cell suspensions were incubated with both BODIPYs at different concentrations, 0.5 and 1.0 μM, for 30 min in the dark at 37 °C. The therapy started upon irradiation with visible light. The viability of *S. aureus* cells after different irradiation times are shown in Figure 8A. Control tests showed that the viability of *S. aureus* was not affected by irradiation of the cells without PS (Figure 8A) or by dark incubation of bacteria with BODIPYs for 30 min (Figure S6A). These results indicate that the inactivation of *S. aureus* found in

cells treated with PS and irradiated was produced by the photosensitization effect of BODIPYs. As shown in Figure 8A, photokilling of *S. aureus* cells was dependent on BODIPY concentrations and irradiation times. A lower *S. aureus* inactivation was found for cells treated with 1 μM BDP 1, reaching 0.5 log and 2.8 log reduction in bacterial survival after 5 min and 15 min light irradiation, respectively. In contrast, cell survival was rapidly decreased for bacteria incubated with BDP 2 and exposed to visible light. Thus, bacterial suspensions treated with 0.5 μM BDP 2 produced 4.5 log decrease in viability with only 2 min of irradiation. Furthermore, no colony formation was found after an exposure of 15 min, indicating that this PS was very effective at concentrations as low as nanomolar. When 1.0 μM BDP 2 was used, complete eradication of *S. aureus* was obtained after 5 min irradiation. Therefore, BDP 2 showed an outstanding inactivation at short irradiation times and low concentrations. PDI mediated by BDP 2 can be compared with other PSs using under similar conditions. Structurally related non-brominated cationic BODIPYs were investigated against *S. aureus* [16]. These PSs inactivated 4 log at 1.0 μM BODIPY after illumination with visible light for 5 min but using a cell density of $1x10^7$ CFU/mL. Similar results were obtained with a porphyrin and its chlorin analog substituted by four dimethylaminopropoxy groups using 1.0 μM PS and 5 min irradiation [17]. With the same conditions, comparable photokilling was also obtained in the presence of a bacteriochlorin bearing two spermine units [34].

On the other hand, PDI studies with BDP 1 and BDP 2 were performed in *E. coli* microbial cells. This Gram-negative bacterium was selected due to the increased antibiotic resistance of *E. coli* cells that have produced a substantial increase in serious infection diseases and considerable spending on public health care [35,36]. Therefore, *E. coli* cells were treated with BODIPYs, using different concentrations of 0.5, 1.0 and 5.0 μM, for 30 min in the dark at 37 °C. After that, bacterial cells were irradiated for different times (5, 15 and 30 min). The survival curves of *E. coli* are shown in Figure 8B. Control experiments indicates that the viability of *E. coli* was not modified by irradiation of cells alone (Figure 8B) or by incubation with PSs in the dark for 30 min (Figure S6B). Thus, the BODIPY-induced photodynamic action was responsible for the cell death of *E. coli*. As

can be seen in Figure 8B, the PDI results indicated that BDP 1 was less active than BDP 2 to photoinactivate *E. coli*. After 30 min irradiation, it was found a reduction of 1.6 log and 5 log when the cells were treated with 1 μM and 5 μM BDP 1, respectively. On the other hand, bacterial suspensions treated with 1.0 μM BDP 2 and irradiated for 5 min produced 4 log decrease in viability, while 15 min irradiation exhibited a photosensitizing activity of 6 log units. These results indicate a cellular inactivation greater than 99.9999%. After 30 min light, bacteria were eradicated and cell viability was not detected. When 5.0 μM BDP 2 was used, with only 15 min of irradiation the *E. coli* cells were eliminated. Furthermore, PDI experiments were also tested with 0.5 μM BDP 2 (Figure S7). Using this low concentration, it was possible to achieve inactivation of 4.5 log (99.997% photokilling) after exposure to visible light of 30 min, demonstrating the high effectiveness of this BODIPY. In previous studies, cationic BODIPYs without bromine atoms were little effective to inactivate *E. coli* [16]. Under similar conditions, a cationic BODIPY contains a *N,N,N*-trimethylamino group attached to the phenylene unit was able to produce a reduction of 2 log, when the cells were treated with 5 μM and 15 min irradiation. Similar result was also obtained with a BODIPY unsubstituted by methyl groups at the *s*-indacene ring and bearing a cationic dimethylaminopropoxy substituent. These non-brominated BODIPYs achieved 4.5 log decrease in *E. coli* survival after 30 min irradiation. The photokilling capacity of these BODIPYs was potentiated by the addition of potassium iodine. Moreover, BDP 2 has shown to be more effective than other PS such as chlorins or porphyrins containing up to four basic amino groups in the periphery to inactivate the same bacterial strain [17]. It was even more effective than a bacteriochlorin substituted by eight aliphatic amine groups [34]. In addition, it was established that a porphyrin substituted by dimethylaminopropoxy groups without intrinsic charges was equally active as its analogous cationic porphyrin in photo-inactivating microorganisms [37,38]. Therefore, the presence of a precursor group of positive charge should be considered to design effective brominated BODIPYs to kill bacteria.

Comparing cell photoinactivation, *S. aureus* was more susceptible than the *E. coli* to the photodynamic effect sensitized by BDP 1 and BDP 2. This different behavior between the two strains can be understood taking into account the structural characteristics of the cell envelope. The cell wall of Gram-positive bacteria is made of multiple layers of peptidoglycan that contain lipoteichoic and teichoic acids [39]. This structural organization gives permeability to the bacterial wall, which facilitates the binding of PS, increasing its photodynamic action that inactivates *S. aureus* [40]. The presence of the OM in Gram-negative bacteria that is located outside the peptidoglycan layer presents an asymmetric lipid structure formed by negatively charged lipopolysaccharides (LPS), lipoproteins and proteins with porin function. Consequently, the OM acts as an effective barrier that is relatively impermeable to neutral or anionic agents. Therefore, PSs substituted by cationic charge precursor groups, such as BDP 2, can interact effectively with the negatively charged outer surface of Gram-negative bacteria, increasing the photoinactivation of *E. coli*.

4. Conclusions

In this work, we presented the synthesis of two new BODIPY derivatives (BDP 1 and BDP 2) containing a dimethylaminopropoxy group attached to the phenylene unit at the *meso*-position of the *s*-indacene ring. Both BODIPYs absorb intensively in the central region of the visible spectrum. In solution, BDP 1 was characterized by an intense green fluorescence emission, very low $O_2(^1\Delta_g)$ production and appreciable ability to form generation $O_2^{\bullet-}$ in presence of β-NADH as reductant. In contrast, brominated BDP 2 showed a low emission of fluorescence with an increased formation of $O_2(^1\Delta_g)$ and less capacity to form $O_2^{\bullet-}$ than BDP 1. Therefore, the photodynamic activity sensitized by BDP 2 involves mainly a type II photoprocess, while in BDP 1 prevails a pathway type I. Binding of these BDIPYs to bacterial cells was rapid, reaching a maximum value at short incubation times. Moreover, BDP 1 showed interesting properties as fluorescent probe for imaging bacterial cells. In PDI studies, *S. aureus* was eliminated when cells were treated with 1 μM of BDP

2 and 5 min irradiation. Furthermore, a higher photokilling was found in *E. coli* after irradiation for 15 min. Therefore, BDP 2 completes the main requirements as a phototherapeutic agent to be used in PDI, such as a short binding time, low concentrations, and short irradiation periods. These BODIPYs contain a dimethylaminopropoxy and its protonation in water allows to increase the binding to the bacterial cells. Moreover, the effect of heavy atom in BDP2 led to an enhance in the photodynamic activity, turning it into a highly effective broad-spectrum antimicrobial phototherapeutic agent.

Acknowledgements

This research was funded by ANPCYT (PICT-2016 0667 and PICT-2017 2404,) and MINCyT Córdoba (PID-2018 36 and GRFT-2018 79). J.E.D., E.N.D. and A.M.D. are Scientific Members of CONICET. Y.B.P. and S.C.S. thank ANPCYT and CONICET for the research fellowships.

Conflict of interest

The authors declare no competing financial interests.

Supporting Information

Additional data including general equipment, experimental procedures and supporting figures.

References

[1] M. N. Ragheb, M. K. Thomason, C. Hsu, P. Nugent, J. Gage, A. N. Samadpour, A. Kariisa, C. N. Merrikh, S. I. Miller, D. R. Sherman, H. Merrikh, Inhibiting the evolution of antibiotic resistance, *Mol. Cell* **2019**, *73*, 157-165.

[2] J. Bengtsson-Palme, E. Kristiansson, D. G. J. Larsson, Environmental factors influencing the development and spread of antibiotic resistance, *FEMS Microbiol. Rev.* **2018**, *42*, 68-80.

[3] N. K. Shrestha, T. G. Fraser, S. M. Gordon, Methicillin resistance in *Staphylococcus aureus* infections among patients colonized with methicillin-susceptible *Staphylococcus aureus*, *Clin. Microbiol. Infect.* **2019**, *25*, 71-75.

[4] X. Z. Li, P. Plésiat, H. Nikaido, The challenge of efflux-mediated antibiotic resistance in Gramnegative bacteria, *Clin. Microbiol. Rev.* **2015**, *28*, 337-418.

[5] C. Furusawa, T. Horinouchi, T. Maeda, Toward prediction and control of antibiotic-resistance evolution, *Curr. Opin. Biotechnol.* **2018**, *54*, 45-49.

[6] R. Singh, A. P. Singh, S. Kumar, B. S. Giri, K. H. Kim, Antibiotic resistance in major rivers in the world: A systematic review, on occurrence, emergence, and management strategies, *J. Clean. Prod.* **2019**, *234*, 1484-1505.

[7] C. Ghosh, P. Sarkar, R. Issa, J. Haldar, Alternatives to conventional antibiotics in the era of antimicrobial resistance, *Trends Microbiol.* **2019**, *27*, 323-338.

[8] M. R. Hamblin, Antimicrobial photodynamic inactivation: A bright new technique to kill resistant microbes, *Curr. Opin. Microbiol.* **2016**, *33*, 67-73.

[9] K. Szaciłowski, W. Macyk, A. Drzewiecka-Matuszek, M. Brindell, G. Stochel, Bioinorganic photochemistry: frontiers and mechanisms, *Chem. Rev.* **2005**, *105*, 2647-2694.

[10] P. R. Ogilby, Singlet oxygen: there is still something new under the sun, and it is better than ever *Photochem. Photobiol. Sci.* **2010**, *9*, 1543-1560.

[11] A. M. Durantini, D. A. Heredia, J. E. Durantini, E. N. Durantini, BODIPYs to the rescue: Potential applications in photodynamic inactivation, *Eur. J. Med. Chem.* **2018**, *144*, 651-661.

[12] N. Boens, B. Verbelen, W. Dehaen, Postfunctionalization of the BODIPY core: synthesis and spectroscopy, *Eur. J. Org. Chem.* **2015**, *30*, 6577-6595.

[13] J. Bañuelos, BODIPY dye, the most versatile fluorophore ever? *Chem. Rec.* **2016**, *16*, 335-348.

[14] M. L. Agazzia, M. B. Ballatorea, A. M. Durantini, E. N. Durantini, A. C. Tomé, BODIPYs in antitumoral and antimicrobial photodynamic therapy: An integrating review, *J. Photochem. Photobiol. C: Photochem. Rev.* **2019**, *40*, 21-48.

[15] M. L. Agazzi, M. B. Ballatore, E. Reynoso, E. D. Quiroga, E. N. Durantini, Synthesis, spectroscopic properties and photodynamic activity of two cationic BODIPY derivatives with application in the photoinactivation of microorganisms, *Eur. J. Med. Chem.* **2017**, *126*, 110-121.

[16] E. Reynoso, E. D. Quiroga, M. L. Agazzi, M. B. Ballatore, S. G. Bertolotti, E. N. Durantini, Photodynamic inactivation of microorganisms sensitized by cationic BODIPY derivatives potentiated by potassium iodide, *Photochem. Photobiol. Sci.* **2017**, *16*, 1524-1536.

[17] D. D. Ferreyra, E. Reynoso, P. Cordero, M. B. Spesia, M. G. Alvarez, M. E. Milanesio, E. N. Durantini, Synthesis and properties of 5,10,15,20-tetrakis[4-(3-*N*,*N*-dimethylaminopropoxy)phenyl] chlorin as potential broad-spectrum antimicrobial photosensitizers. *J. Photochem. Photobiol. B: Biol.* **2016**, *158*, 243-251.

[18] A. C. Scanone, N. S. Gsponer, M. G. Alvarez, E. N. Durantini, Porphyrins containing basic aliphatic amino groups as potential broadspectrum antimicrobial agents, *Photodiagn. Photodyn. Ther.* **2018**, *24*, 220-227.

[19] A. M. Durantini, L. E. Greene, R. Lincoln, S. R. Martínez, G. Cosa, Reactive oxygen species mediated activation of a dormant singlet oxygen photosensitizer: from autocatalytic singlet oxygen amplification to chemicontrolled photodynamic therapy, J. Am. Chem. Soc. **2016**, *138*, 1215-1225.

20 M. L. Agazzi, J. E. Durantini, N. S. Gsponer, A. M. Durantini, S. G. Bertolotti, E. N. Durantini, Light-harvesting antenna and proton-activated photodynamic effect of a novel BODIPY-fullerene C_{60} dyad as potential antimicrobial agent, *ChemPhysChem* **2019**, *20*, 1110-1125.

[21] S. R. Martínez, Y. B. Palacios, D. A. Heredia, M. L. Agazzi, A. M. Durantini, Phenotypic resistance in photodynamic inactivation unravelled at the single bacterium level, *ACS Infect. Dis.* **2019**, *5*, 1624-1633.

[22] A. C. Scanone, S. C. Santamarina, D. A. Heredia, E. N. Durantini, A. M. Durantini, Functionalized magnetic nanoparticles with BODIPYs for bioimaging and antimicrobial therapy applications, *ACS Appl. Bio Mater.* **2020**, *3*, 1061-1070.

[23] de Rezende L.C.D., da Silva Emery F., A review of the synthetic strategies for the development of BODIPY dyes for conjugation with proteins, *Orbital Elec. J. Chem.* **2013**, *5*, 62-83.

24 L. Wang, J. W. Wang, A. J. Cui, X. X. Cai, Y. Wan, Q. Chen, M. Y. He, W. Zhang, Regioselective 2,6-dihalogenation of BODIPYs in 1,1,1,3,3,3-hexafluoro-2-propanol and preparation of novel meso-alkyl polymeric BODIPY dyes, *RSC Adv.* **2013**, *3*, 9219-9222.

[25] A.V. Rayer, K.Z. Sumon, L. Jaffari, A. Henni, Dissociation constants (pK_a) of tertiary and cyclic smines: Structural and temperature dependences, *J. Chem. Eng. Data* **2014**, *59*, 3805-3813.

[26] H. Lu, J. Mack, T. Nyokong, N. Kobayashi, Z. Shen, Optically active BODIPYs, *Coord. Chem. Rev.* **2016**, *318*, 1-15.

[27] J. Wang, Y. Hou, W. Lei, Q. Zhou, C. Li, B. Zhang, X. Wang, DNA photocleavage by a cationic bodipy dye through both singlet oxygen and hydroxyl radical: new insight into the photodynamic mechanism of BODIPYs, *ChemPhysChem* **2012**, *13*, 2739-2747.

[28] H. L. Kee, C. Kirmaier, L. Yu, P. Thamyongkit, W. J. Youngblood, M. E. Calder, L. Ramos, B. C. Noll, D. F. Bocian, W. R. Scheidt, R. R. Birge, J. S. Lindsey, D. Holten, Structural control of the photodynamics of boron-dipyrrin complexes, *J. Phys. Chem. B* **2005**, *109*, 20433-20443.

[29] A. Harriman, L. J. Mallon, G. Ulrich, R. Ziessel, Rapid intersystem crossing in closely-spaced but orthogonal molecular dyads, *ChemPhysChem* **2007**, *8*, 1207-1214.

[30] J. Zhao, K. Xu, W. Yang, Z. Wang, F. Zhong, The triplet excited state of Bodipy: formation, modulation and application, *Chem. Soc. Rev.* **2015**, *44*, 8904-8939.

[31] A. Gomes, E. Fernandes, J. L. F. C. Lima, Fluorescence probes used for detection of reactive oxygen species, *J. Biochem. Biophys. Methods* **2005**, *65*, 45-80.

[32] N. S. Gsponer, M. B. Spesia, E. N. Durantini, Effects of divalent cations, EDTA andchitosan on the uptake and photoinactivation of *Escherichia coli* mediated by cationic and anionic porphyrins, *Photodiagn. Photodyn. Ther.* **2015**, *12*, 67-75.

[33] R. J. Melander, C. Melander, The challenge of overcoming antibiotic resistance: an adjuvant approach?, *Infect. Dis.* **2017**, *3*, 559-563.

[34] M. B. Ballatore, M. E. Milanesio, H. Fujita, J. S. Lindsey, E. N. Durantini, Bacteriochlorin-bis(spermine) conjugate affords an effective photodynamic action to eradicate microorganisms, *J. Biophotonics* **2020**, *13*, e201960061.

[35] Y. Chong, S. Shimoda, N. Shimono, Current epidemiology, genetic evolution and clinical impact of extended-spectrum β-lactamase-producing *Escherichia coli* and *Klebsiella pneumoniae*, *Infect. Genet. Evol.* **2018**, *61*, 185-188.

[36] A. Mirhoseini, J. Amani, S. Nazarian, Review on pathogenicity mechanism of enterotoxigenic *Escherichia coli* and vaccines against it, *Microb. Pathog.* **2018,** *117*, 162-169.

[37] E. D. Quiroga, S. J. Mora, M. G. Alvarez, E. N. Durantini, Photodynamic inactivation of *Candida albicans* by a tetracationictentacle porphyrin and its analogue without intrinsic charges in presence of fluconazole, *Photodiagn. Photodyn. Ther.* **2016**, *13*, 334-340.

[38] E. D. Quiroga, P. Cordero, S. J. Mora, M. G. Alvarez, E. N. Durantini, Mechanistic aspects in the photodynamic inactivation of *Candida albicans* sensitized by a dimethylaminopropoxy

porphyrin and its equivalent with cationic intrinsic charges, *Photodiagn. Photodyn. Ther.* **2020**, *31*, 101877.

[39] N. Malanovic, K. Lohner, Gram-positive bacterial cell envelopes: the impact on the activity of antimicrobial peptides, *Biochim. Biophys. Acta-Biomembranes* **2016**, *1858*, 936-946.

[40] Y. Y. Huang, S. K. Sharma, R. Yin, T. Agrawal, L. Y. Chiang, M. R. Hamblin, Functionalized fullerenes in photodynamic therapy, *J. Biomed. Nanotech.* **2014**, *10*, 1918-1936.

Table 1. Spectroscopic and photodynamic properties of BDP 1 and BDP 2 in ACN.

BODIPY	λ_{abs}^{max} (nm)	$\varepsilon^{max\ a}$	λ_{em}^{max} (nm)	E_s (eV)	Φ_F [b]	k_{obs}^{DMA} (s^{-1}) [c]	Φ_Δ [d]
BDP 1	497	9.1×10^4	506	2.47	0.85 ± 0.02	$(5.45 \pm 0.05) \times 10^{-5}$	0.014 ± 0.005
BDP 2	522	8.9×10^4	537	2.34	0.24 ± 0.01	$(1.81 \pm 0.02) \times 10^{-3}$	0.51 ± 0.02

[a] molar absorption coefficient (L mol^{-1} cm^{-1}), [b] fluorescence quantum yield using H_2B-OAc as a reference [19], [c] observed rate constants for the photooxidation reaction of DMA, [d] quantum yield of $O_2(^1\Delta_g)$ production using Br_2B-OAc as a reference $k_{obs}^{ACN} = (2.\text{X} \pm 0.02) \times 10^{-3}$ s^{-1} and $\Phi_\Delta^{ACN} = 0.79$ from ref. [19].

Figures and Schemes captions

Figure 1. The structures optimized by DFT / TD-DFT and the ESP surfaces of the BDP 1 and BDP 2 molecules and their protonated forms (BDP 1-H^+ and BDP 2-H^+). The negative ESP regions was shown in red and the positive regions in blue.

Figure 2. (A) Absorption spectra and (B) fluorescence emission spectra (λ_{exc} = 480 nm) of BDP 1 (dashed line) and BDP 2 (solid line) in ACN.

Figure 3. Optimized structure, highest occupied molecular orbital (HOMO) and lowest unoccupied molecular orbital (LUMO) of the BDP 1 and BDP 2 molecules. All calculations were performed by DFT at the B3LYP/6-31+G(d) level using Gaussian 09.

Figure 4. First-order plots for the photodecomposition of DMA (35 μM) photosensitized by BDP 1 (▼), BDP 2 (▲) and Br_2B-OAc (●) in ACN; λ_{irr} = 506 nm.

Figure 5. Time course of NBT (0.2 mM) reduction to diformazan photosensitized by BDP 1 (▼) and BDP 2 (▲) in presence of β-NADH (0.5 mM); λ_{irr} = 506 nm. Controls: NBT+β-NADH (●), BDP1 + NBT (▽), BDP 2 + NBT (△).

Figure 6. Amount of BODIPY recovered from (A) *S. aureus* (~10^8 CFU/mL) treated with 0.5 μM BDP 1 (▽), 1.0 μM BDP 1 (▼), 0.5 μM BDP 2 (△), 1.0 μM BDP 2 (▲) for different incubation times at 37 ºC in dark.

Figure 7. Bright field images (left) and fluorescence emission images (right) for *S. aureus* (top) and *E. coli* (bottom) cells incubated with 1 μM (A) BDP 1 and (B) BDP2 for 30 min at 37 °C in the dark; 100×microscope objective, scala bar 5 μm.

Figure 8. Survival curves of (A) *S. aureus* (~10^8 CFU/mL) incubated with 0.5 μM (▽) and 1.0 μM (▼) of BDP 1 and 0.5 μM (△) and 1.0 μM (▲) of BDP 2 and (B) *E. coli* (~10^8 CFU/mL) incubated with 1.0 μM (▽) and 5.0 μM (▼) of BDP 1 and 1.0 μM (△) and 5.0 μM (▲) of BDP 2 for 30 min at 37 °C in the dark. Samples were irradiated for different periods with visible light. Control cells untreated with PS and irradiated (●).

Scheme 1. Synthesis of BDP 1 and BDP 2.

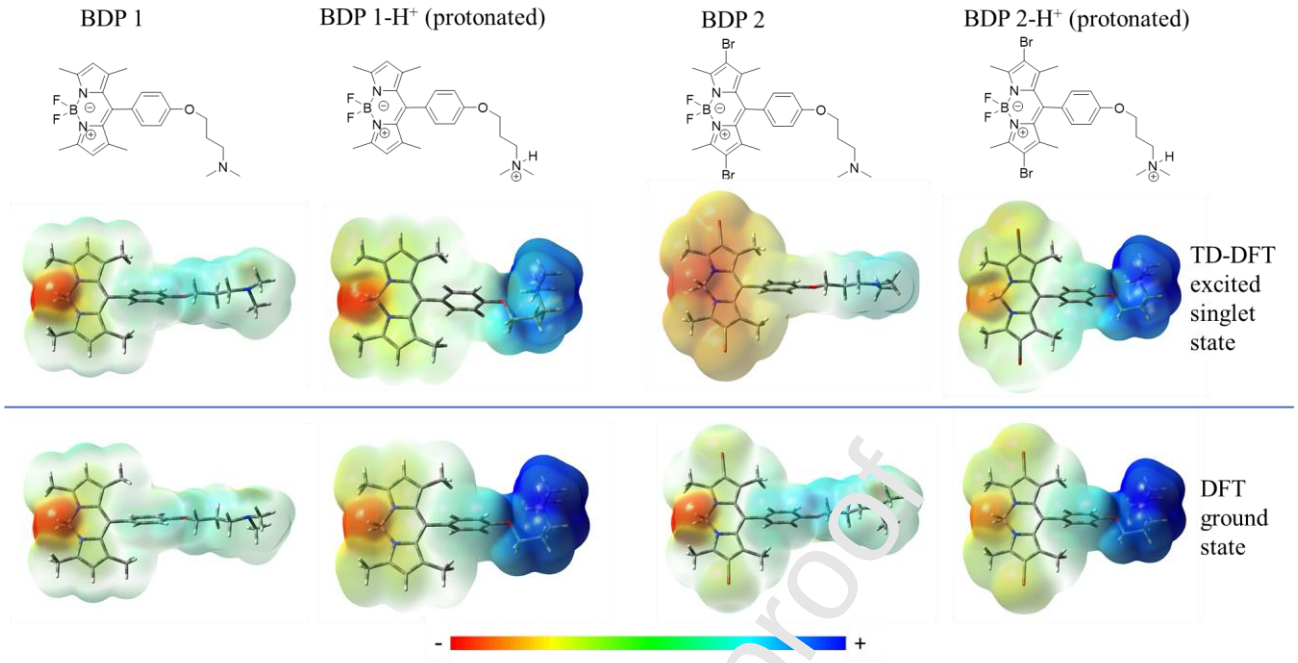

Figure 1

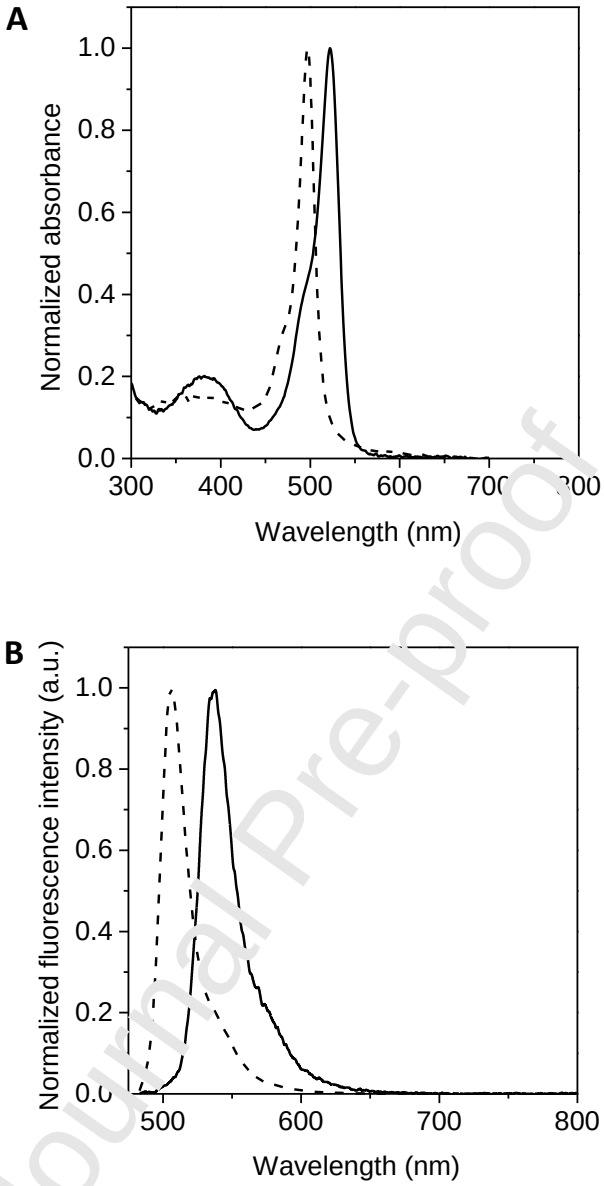

Figure 2

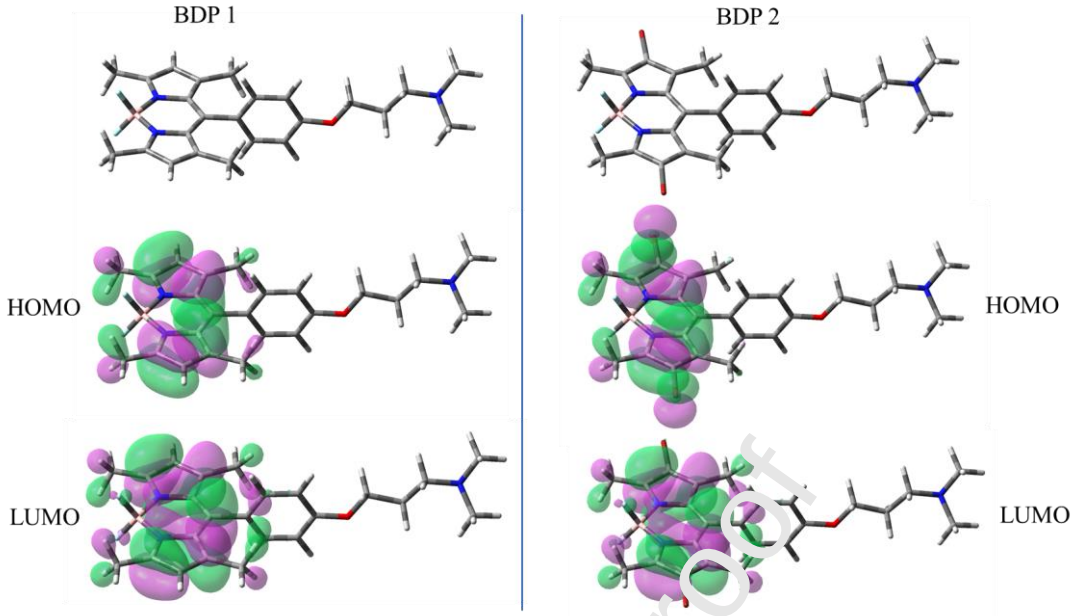

Figure 3

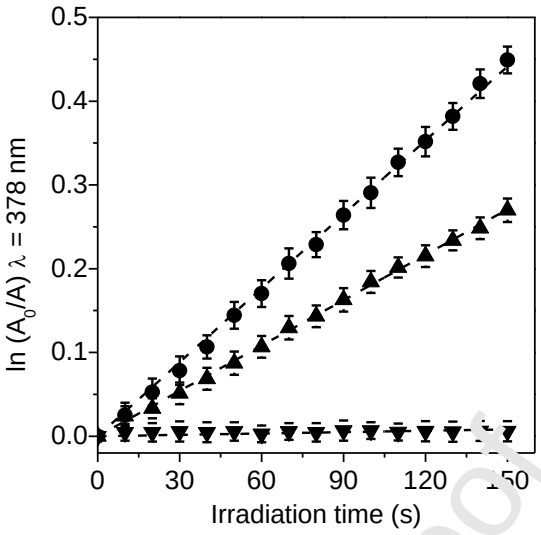

Figure 4

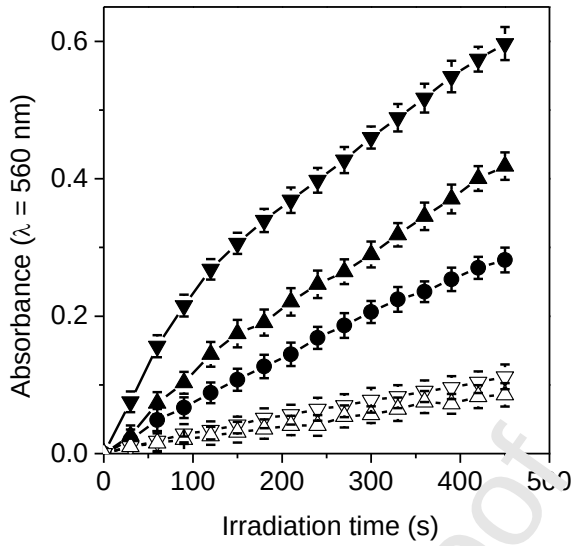

Figure 5

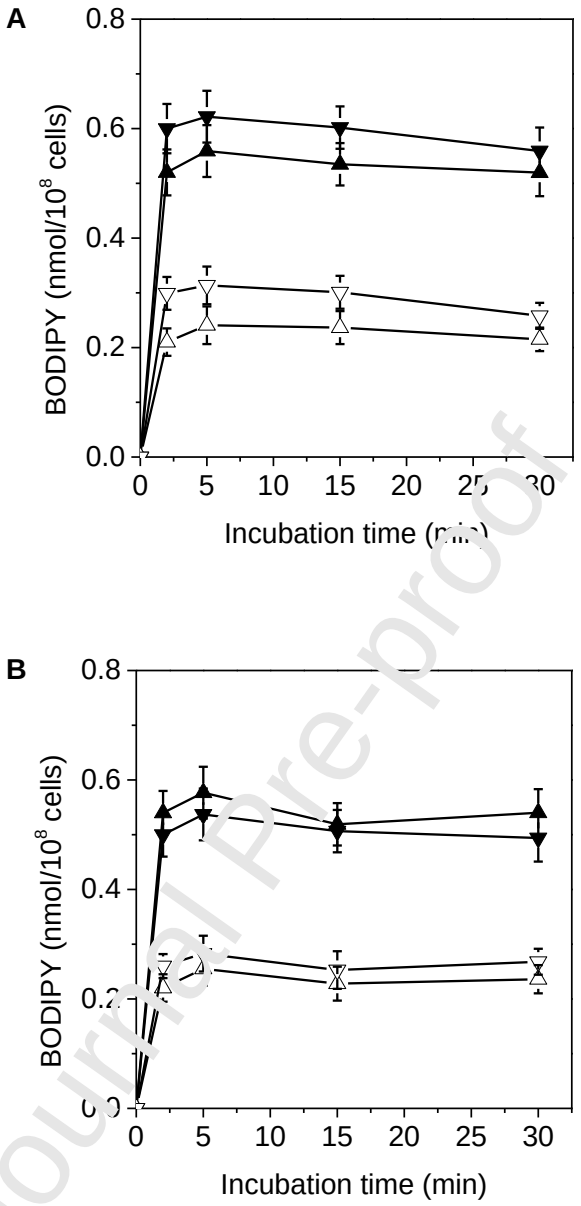

Figure 6

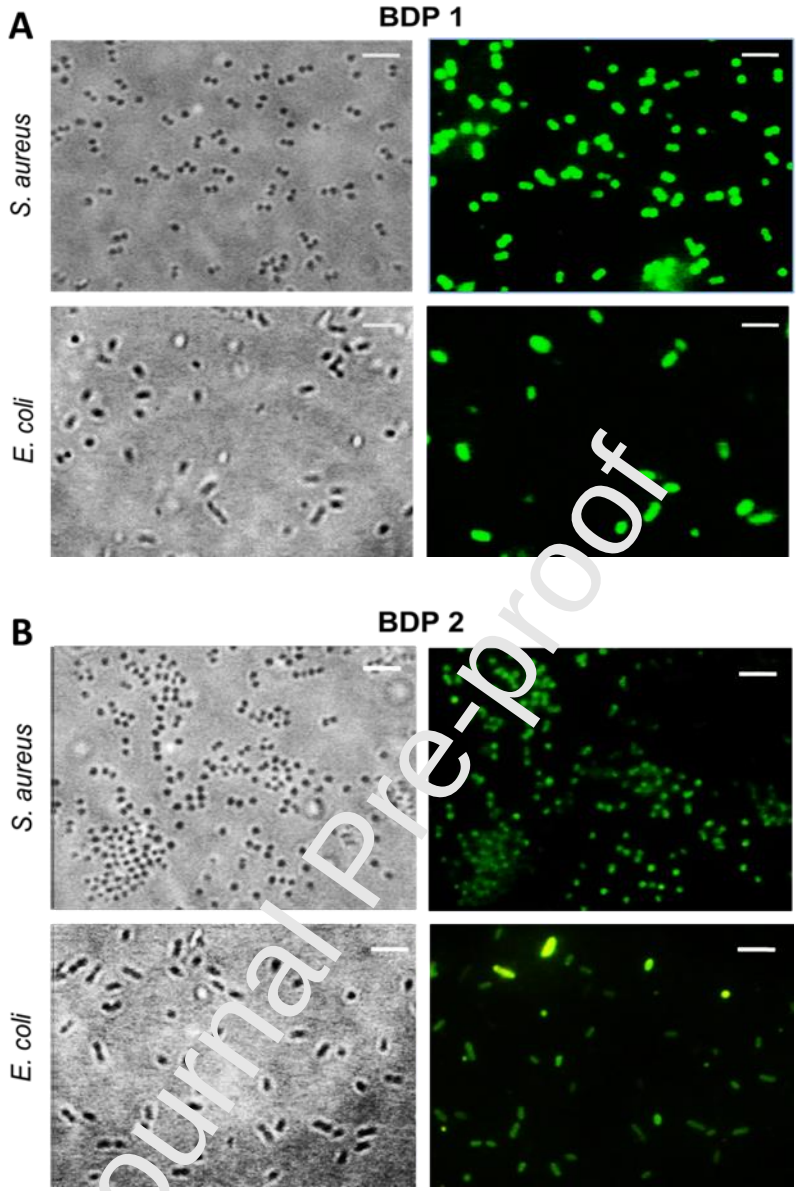

Figure 7

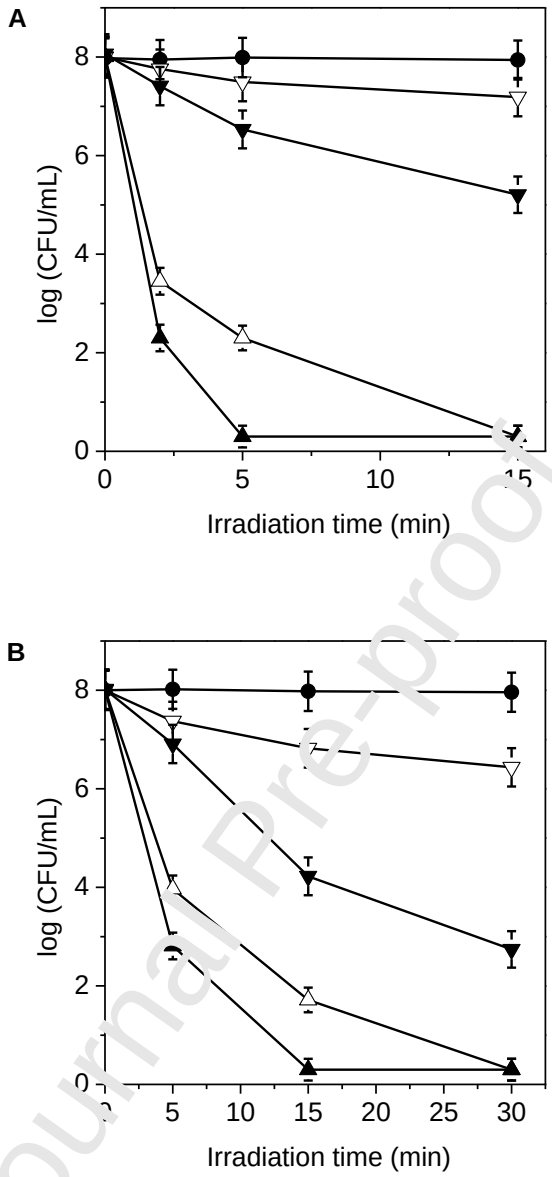

Figure 8

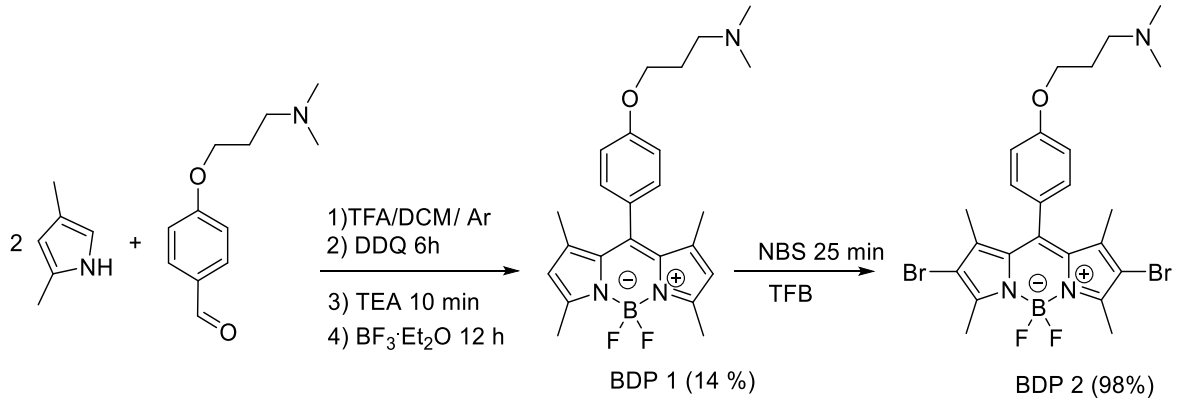

Scheme 1

Declaration of interests

☒ The authors declare that they have no known competing financial interests or personal relationships that could have appeared to influence the work reported in this paper.

☐The authors declare the following financial interests/personal relationships which may be considered as potential competing interests:

Graphical abstract

BODIPY derivatives are a promising molecular architecture for use as a broad-spectrum antimicrobial photosensitizer. The presence of a basic amine group in the BODIPY structure allows a better binding to bacterial cells, leading to a highly effective photoinactivation. This molecular design of a phototherapeutic agent augurs very well for possible future clinical applications.

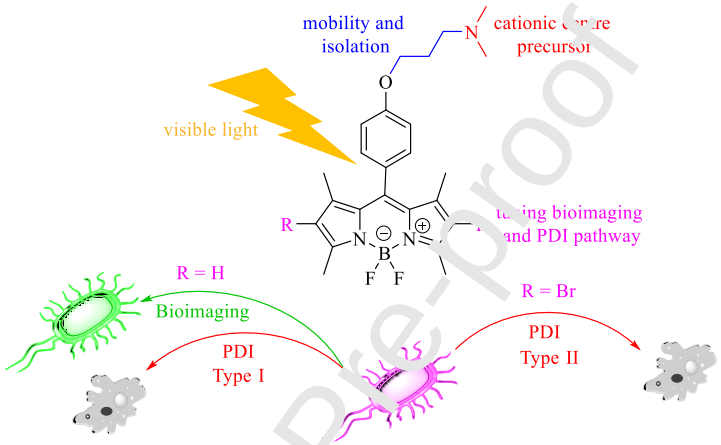

- New BODIPYs containing a dimethylaminopropoxy group were synthesized.
- The basic aliphatic amino group provides effective binding to bacterial cells.
- The highly fluorescent BODIPY is an interesting fluorophore for bioimaging.
- Brominated BODIPY was highly effective to eradicate bacteria at low concentrations.

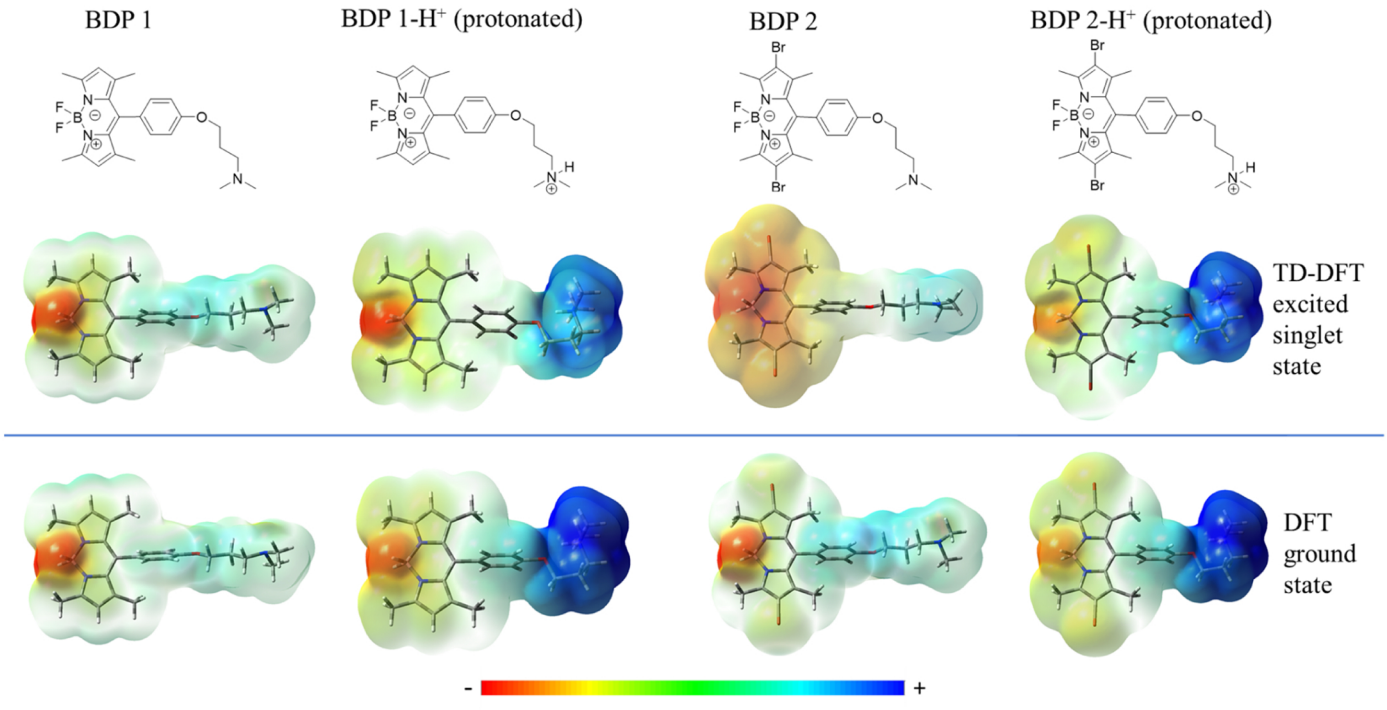
BDP 1
BDP 1-H+ (protonated)
BDP 2
BDP 2-H+ (protonated)
TD-DFT excited singlet state
DFT ground state
-
+

Figure 1

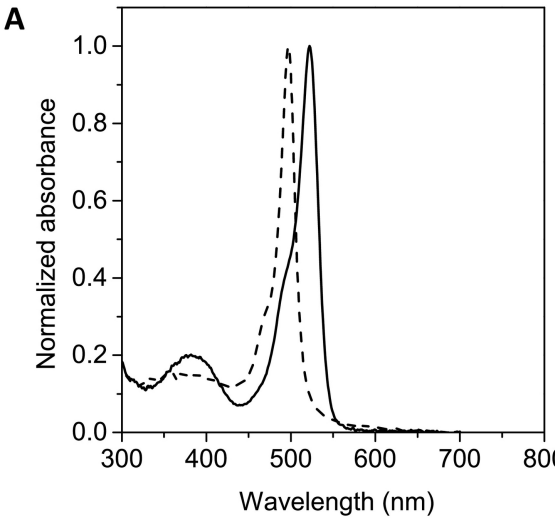
A
Normalized absorbance
1.0
0.8
0.6
0.4
0.2
0.0
300
400
500
600
700
800
Wavelength (nm)

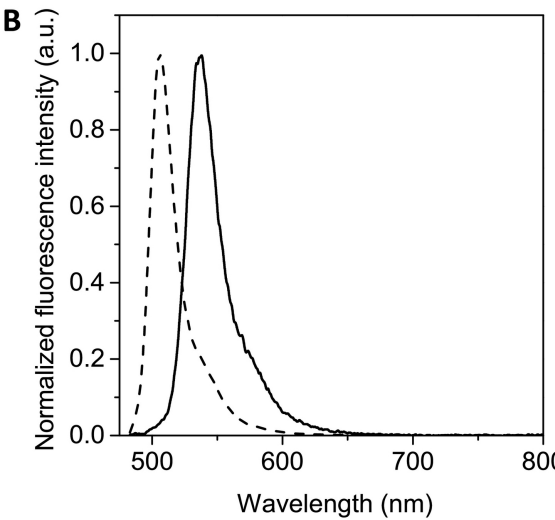
B
Normalized fluorescence intensity (a.u.)
1.0
0.8
0.6
0.4
0.2
0.0
500
600
700
800
Wavelength (nm)

Figure 2

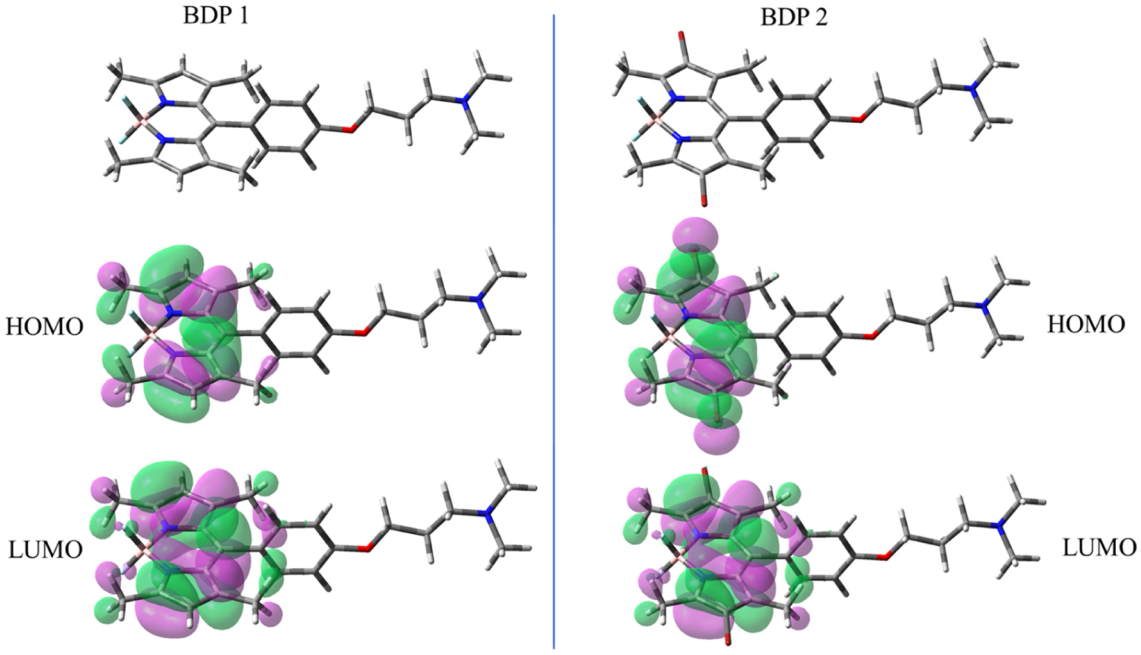

Figure 3

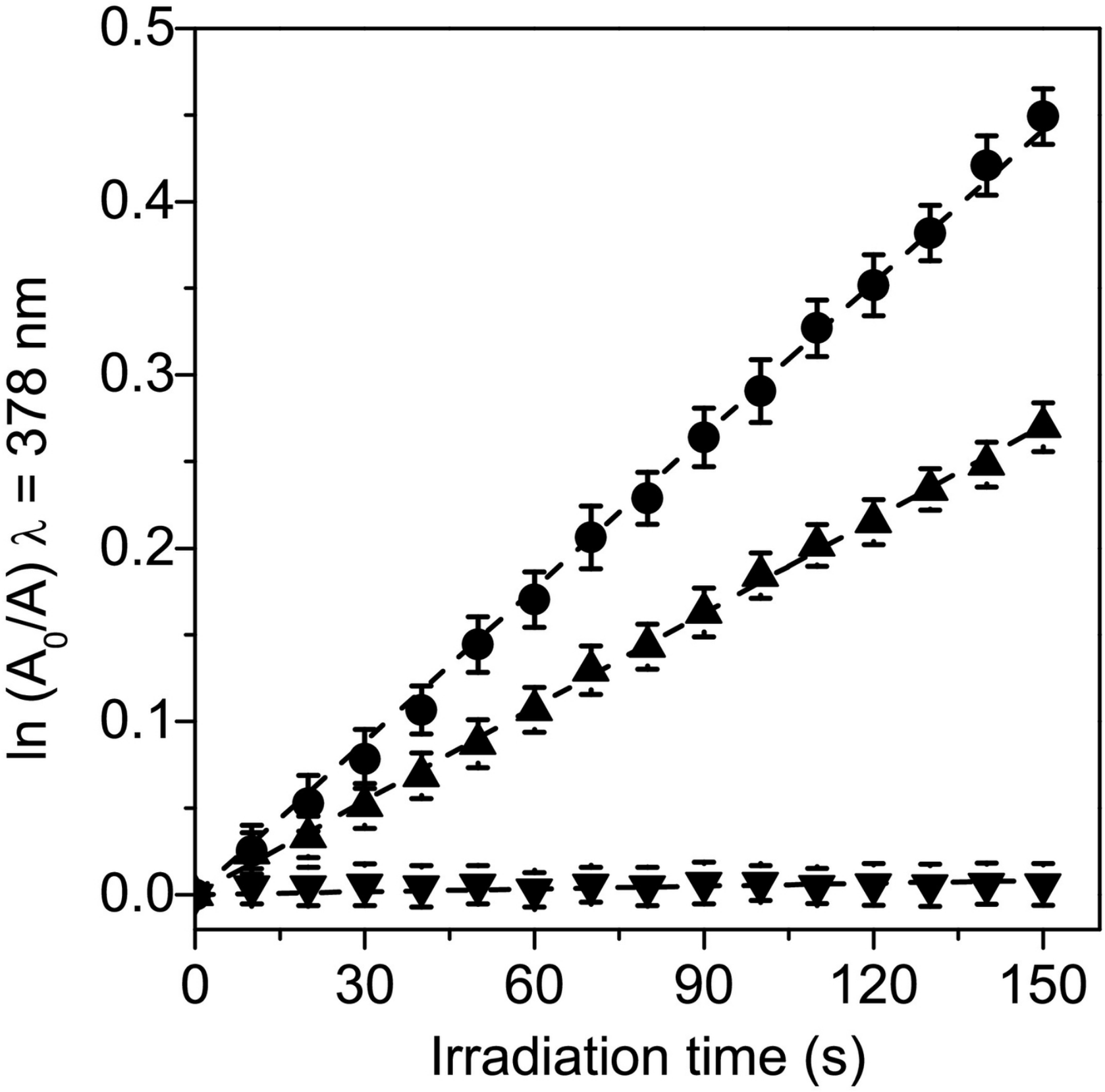
0.5
0.4
0.3
0.2
0.1
0.0
ln (A0/A) λ = 378 nm
0
30
60
90
120
150
Irradiation time (s)

Figure 4

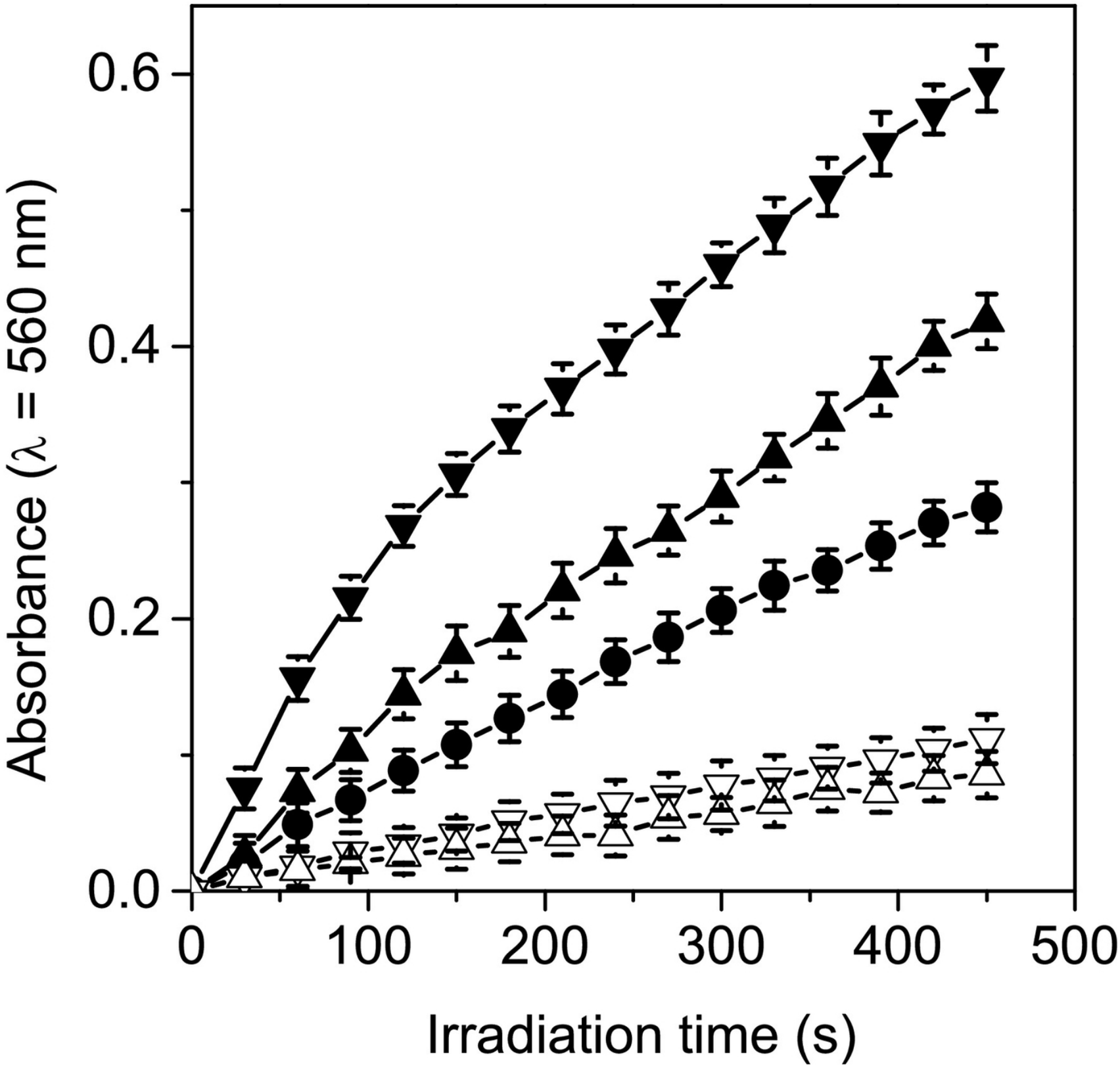
Absorbance (λ = 560 nm)
0.0
0.2
0.4
0.6
0
100
200
300
400
500
Irradiation time (s)

Figure 5

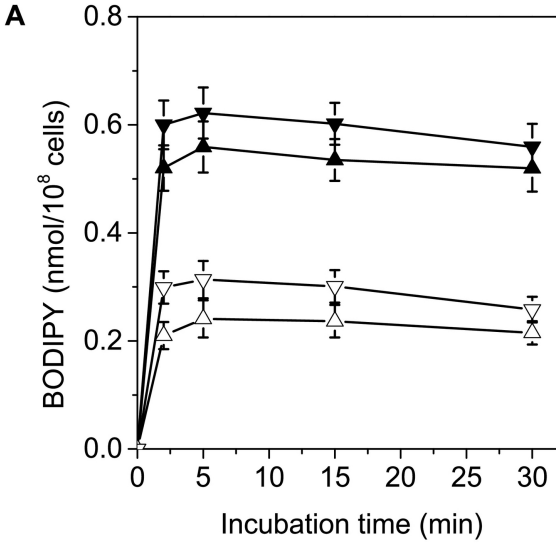
A
0.8
0.6
0.4
0.2
0.0
BODIPY (nmol/10^8 cells)
0
5
10
15
20
25
30
Incubation time (min)

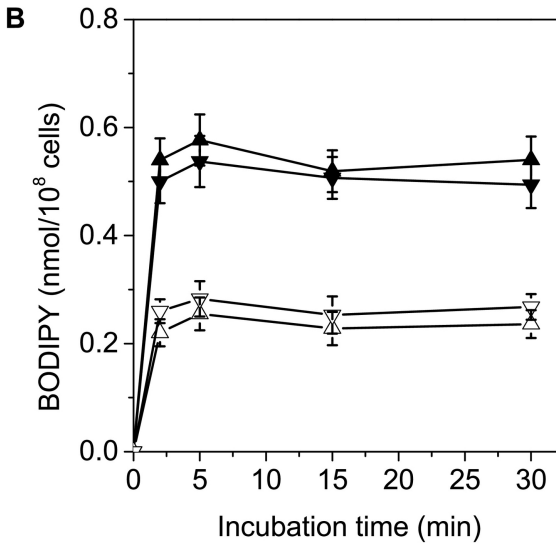
B
0.8
0.6
0.4
0.2
0.0
BODIPY (nmol/10^8 cells)
0
5
10
15
20
25
30
Incubation time (min)

Figure 6

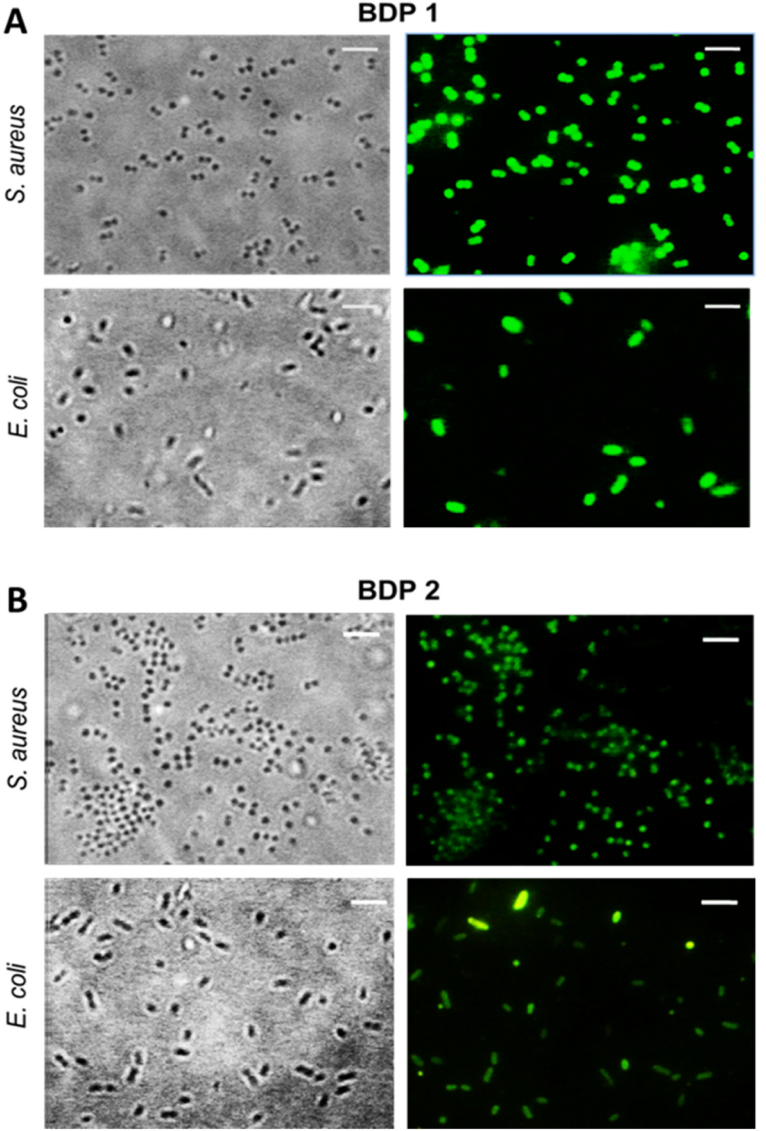

Figure 7

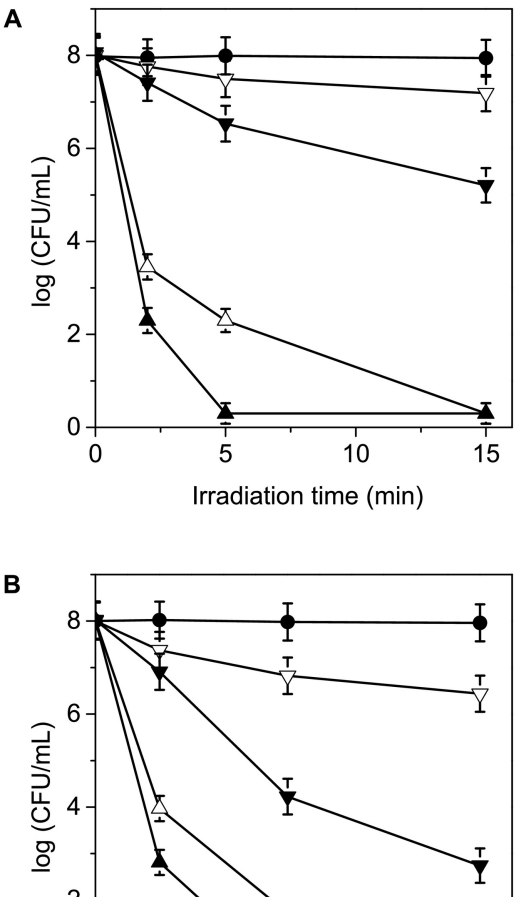
A
log (CFU/mL)
0
2
4
6
8
0
5
10
15
Irradiation time (min)
B
log (CFU/mL)
0
2
4
6
8
0
5
10
15
20
25
30
Irradiation time (min)

Figure 8